J. theor. Biol. (1983) **101**, 387–400

Lineweaver–Burk, Hanes, Eadie–Hofstee and Dixon Plots in Non-steady-state Situations

JEAN-MARIE FRÈRE†, BERNARD LEYH AND ANDRÉ RENARD

Services de Microbiologie et de Biochimie, Université de Liège, Institut de Chimie, B6, B-4000 Sart Tilman (Liège), Belgium

(*Received* 15 *February* 1982, *and in revised form* 26 *October* 1982)

Lineweaver–Burk, Hanes, Eadie–Hofstee and Dixon plots can only be used when a true initial rate is measured. Despite the fact that this point has often been stressed, it is far too often ignored in favour of restricting the assay time to one where low amounts of substrate are used. When one or several irreversible and slow steps occur with an inactivator during the incubation of a ternary enzyme-substrate-inactivator mixture, the rate of the enzyme-catalysed reaction progressively decreases. Even under these conditions, the present computer simulations investigations show that apparently linear Lineweaver–Burk, Hanes, Eadie–Hofstee and Dixon graphs can be obtained when the amount of product formed is mistakenly assumed to represent the true initial rate. Moreover, the observed pattern can change with time, going for instance from non-competitive to competitive. "Ki's" measured under these conditions also vary with time and bear little relationship to the true constants involved in the interaction.

The measurement of a true steady-state (or initial) velocity is a prerequisite for obtaining meaningful Lineweaver–Burk, Hanes, Eadie–Hofstee and Dixon plots. Despite the fact that this point has often been made, it is quite often ignored in favour of restricting the assay time to conditions where low amounts of substrate are used. If the appearance of product or the disappearance of substrate cannot be continuously monitored, conditions are usually chosen in which a maximum of 10–15% (in an irreversible reaction) of substrate is consumed.

Lineweaver–Burk and Dixon plots have been used by several authors (including one of us), in the study of the inhibition of penicillin-sensitive, D-alanyl-D-alanine carboxy- and transpeptidases by β-lactam antibiotics (Izaki & Strominger, 1968; Leyh-Bouille *et al.*, 1971, 1972; Barnett, 1973; Umbreit & Strominger, 1973; Frère *et al.* 1974*b*; Oppenheim, Koren & Patchornik, 1974; Yocum, Blumberg & Strominger, 1974; Martin, Maskos

† To whom correspondence should be sent.

0022–5193/83/070387 + 14 $03.00/0

& Burger, 1975). At least with some of these enzymes, the enzyme-β-lactam interaction was first thought to be a rapid equilibrium. In all experiments, the reaction was stopped after a very small proportion of the peptide substrate (R-D-alanyl-D-alanine) had been hydrolyzed. It was then assumed that the initial rate conditions were fulfilled, and a "steady-state" velocity was computed on the basis of the amount of D-alanine released at the end of the incubation period (10 to 60 min, depending upon the experiment). In some experiments, the total concentration of benzylpenicillin was not much larger than that of the enzyme (the D-alanyl-D-alanine peptidase of *Streptomyces* R61) and the data were analyzed using the Henderson–Morrison equation for tight-binding inhibitors (Morrisson, 1969; Henderson, 1972).

The steady-state assumption, however, turned out to be wrong: it was found that the interaction between enzymes (E) and penicillins (I) obeyed a three-step mechanism:

$$E + I \overset{K}{\rightleftharpoons} EI \xrightarrow{k_2} EI^* \xrightarrow{k_3} E + I^*(s) \qquad (1)$$

where K is the dissociation constant of EI, and k_2 and k_3 are first-order rate constants (Frère, Ghuysen & Iwatsubo, 1975*a*). The third step (k_3) regenerated native enzyme and one or more irreversibly altered, inactive metabolites [$I^*(s)$] were released. The antibiotic molecule was sometimes fragmented (Frère. *et al.*, 1975*c*). After the various constants along the pathway were measured, it became evident that, in the first experiments, the inactivated complex EI^* had slowly and progressively accumulated during the incubation of the ternary mixture (enzyme + substrate + inhibitor) (Frère, Ghuysen & Perkins, 1975*b*), inducing a corresponding decrease in reaction rate.

Surprisingly, at least for us, the Lineweaver–Burk, Henderson–Morrisson, and Dixon plots which had been erroneously constructed with these data were, within the limits of experimental errors, perfectly linear and no indication of an abnormal situation was obtained from a careful examination of the plots (Leyh-Bouille *et al.*, 1971; Frère *et al.*, 1974*a*). The only exception was the DD-carboxypeptidase-transpeptidase of *Actinomadura* R39, for which the Dixon plots were non-linear, but it could easily be demonstrated that the observed curves were due to a simple titration effect (Frère *et al.* 1974*b*).

After the experimental demonstration of the validity of scheme (1), it was possible to propose a general model for the interaction between enzyme, inhibitor and substrate (Frère *et al.* 1975*b*).

$$\begin{array}{ccccc} E+I & \overset{K}{\rightleftharpoons} & EI & \xrightarrow{k_2} & EI^* \xrightarrow{k_3} E+I^*(s) \\ {\scriptstyle Km}\,\Big\updownarrow{\scriptstyle +S} & & \Big\updownarrow{\scriptstyle K'm} & & \\ ES+I & \underset{K'}{\rightleftharpoons} & ESI & & \\ {\scriptstyle k}\,\Big\downarrow & & & & \\ E+P & & \text{where } \dfrac{K'm}{Km}=\dfrac{K'}{K}=q & & \end{array} \qquad (2)$$

In this scheme, the four steps in the loop are assumed to be in rapid equilibrium and $k = k_{cat}$.

If P represents the amount of product formed from substrate S at time t ($P = k\int_0^t [ES]\,dt$), and P_M ($P_M = kE_0t$), the amount of product formed at maximum velcocity, the ratio P/P_M can be computed as the algebraic sum of three terms:

$$\frac{P}{P_M}=\frac{\int_0^t [ES]\,dt}{E_0t}=l+m-n \qquad (3)$$

where

$$l=\frac{k_3}{b(k_3+k_a)} \qquad m=\frac{k_a}{b(k_3+k_a)^2t} \qquad n=\frac{k_a\,e^{-(k_3+k_a)t}}{b(k_3+k_a)^2t}$$

where

$$b=1+\frac{Km}{[S]}\left(1+\frac{[I]}{K}\right)+\frac{[I]}{K'}$$

and

$$k_a=\frac{k_2}{1+\dfrac{K}{[I]}\left(1+\dfrac{[S]}{Km}\right)+\dfrac{[S]}{K'm}}.$$

This general model is non-competitive, but the equation for a competitive model (no ternary complex) is easily obtained by setting K' and $K'm = \infty$ (i.e. by choosing a large value of q). In this case, the rapid equilibrium assumption is no longer necessary in the "substrate branch" and Km and k_{cat} can be assigned their general values.

Equation (3) is comparable to those calculated by Frieden (1970) and Cha (1975) for somewhat different slow systems. Term l represents the contribution of the steady-state conditions to the total amount of product (Fig. 1) and terms m and n represent the non-steady-state contributions. By hypothesis, the steady-state is reached slowly in the interaction between E and I, rapidly in the interaction between E and S.

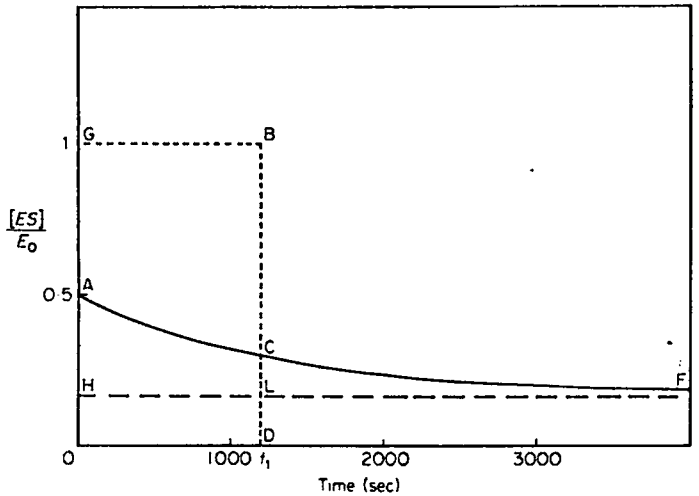

FIG. 1. Illustration of equation (3) for the following conditions. Competitive model, $[S] = Km$, $k_2 = 1\ \text{sec}^{-1}$, $k_3 = 2{\cdot}5 \times 10^{-4}\ \text{sec}^{-1}$, $[I] = K \times 10^{-3}$ (i.e. $z = 0{\cdot}001$). The value of P_M at time t_1 is given by $k_{cat} \times$ the area of the rectangle OGBD; the value of P by $k_{cat} \times$ OACD. The values of the three terms of equation 1 are easily visualized:

$$l = \frac{\text{OHLD}}{\text{OGBD}};\ m = \frac{\text{AHF}}{\text{OGBD}} \text{ and } n = \frac{\text{FCL}}{\text{OGBD}};\ \frac{P}{P_M} = \frac{\text{OACD}}{\text{OGBD}}.$$

For the D-alanyl-D-alanine peptidase of *Streptomyces* R61, the values of Km, K, k_2 and k_3 were obtained from independent experiments. At 37°C, Km was 12 mM for the peptide substrate and, for penicillin V for instance, the following values were found: $k_2/K = 1500\ \text{M}^{-1}\ \text{sec}^{-1}$ (with $K > 1$ mM and $k_2 > 1\ \text{sec}^{-1}$) and $k_3 = 2{\cdot}8 \times 10^{-4}\ \text{sec}^{-1}$.

Equation (3) was then used to compute the value of $(P/P_M)_c$, i.e. the P/P_M ratio which should have been expected in the experiments which had been erroneously considered as steady-state experiments, and this calculated value of $(P/P_M)_c$ was compared to $(P/P_M)_m$, i.e. the value which had been actually obtained in these experiments. The following observations were made: (a) a good agreement was found between $(P/P_M)_c$ and $(P/P_M)_m$; (b) when $(P_M/P)_c$ was plotted vs $1/[S]$ or $[I]$, straight lines were obtained, similar to those recorded when $(P_M/P)_m$ was plotted vs $1/[S]$ or $[I]$; (c) in all cases, the steady-state term l was smaller than the algebraic sum of the two non-steady-state terms $m - n$; (d) $(P/P_M)_c$ was computed using the competitive model, since no indication of a non-competitive model had been found. However, the results did not allow the rejection of a non-competitive model: if one assumed the values of K' and $K'm$ to be similar to those of K and Km, respectively, identical values of $(P/P_M)_c$ were found.

This was due to the fact that, since $[I]$ was always much smaller than K, the observed inhibition was only due to the accumulation of EI^*. In other words, $[EI]$ and $[ESI]$ always remained negligible when compared to $[EI^*]$.

Linear plots of $1/P$ vs $1/[S]$ were also obtained by Cha, Agarwal & Parks (1975) in the study of the interaction between adenosine deaminase, substrate and a slow-binding inhibitor, coformycin.

The present study was undertaken to decide whether the observed apparent linearity of the P_M/P vs $1/[S]$ or $[I]$ plots was a coincidence, due to particular values of the various constants, or if the equations $P_M/P = f(1/[S])$ and $P_M/P = f([I])$ would generate curves very similar to straight lines for other values of the constants, as long as the conditions remained reasonably close to those usually utilized in actual experiments. Moreover, since the double reciprocal plot is notorius at hiding any deviation from linearity, the study was extended to the Hanes ($[S]/v$ vs $[S]$) and Eadie–Hofstee (v vs $v/[S]$) plots.

In practice, we used substrate concentrations ranging from $Km/5$ to $5\,Km$ and inactivator concentrations were chosen so that the ratio P/P_M remained larger than 0·01. In most simulations, conditions were such that P/P_M was larger than 0·05.

Methods

The simulations were made using a Tektronix 4051 computer, equipped with an interactive digital plotter. The program was written in BASIC language.

Lineweaver–Burk plots

P_M/P was plotted vs $1/x$ ($x = [S]/Km$; $1/x$ was varied from 0·2 to 5·0 in 24 increments of 0·2. The maximal value of z ($z = [I]/K$) used in each simulation depended upon the values of the other parameters (i.e. k_2, k_3, q and t); z was varied from 0 to the maximal value in five or six identical increments.

Dixon plots

P_M/P was plotted vs z; z was varied from 0 to the maximal value in 25 identical increments. Six different values of x were used: 4, 2, 1, 0·5, 0·33 and 0·2.

Hanes plots

The Hanes graphs were obtained by plotting $P_M/P \cdot x$ vs x. In this case, $[S]/Km$ was varied from 0·2 to 5.

Eadie-Hofstee plots

The Eadie–Hofstee graphs were obtained by plotting P/P_M vs $P/P_M \cdot 1/x$. The values of x were 0·20, 0·28, 0·36, 0·44, 0·56, 0·71, 0·83, 1·0, 1·25, 1·67, 2·5, 5·0.

Finally, $P_M/P \cdot x$ was also plotted vs z.

PARAMETERS

The values of k_2 were varied from 1×10^{-3} to 200 s^{-1}, those of k_3 from 0 to k_2. The values of q were varied from 10^{-3} to 100 and the time from 30 to 30 000 sec. Since all the combinations could not possibly be tested, the values of the constants were chosen to encompass a wide variety of conditions, from competitive to uncompetitive models, from non-steady-state to steady-state situations and from conditions involving an important accumulation of EI^* to conditions in which EI^* was not the most abundant inactive complex.

RESULTS

VERY HIGH VALUES OF q: COMPETITIVE MODEL ($q = 100$)

The competitive model was simulated using a value of $q = 100$. Larger values of q did not produce significant variations (a truly competitive model implies $q = \infty$). Situations in which EI^* did not decay ($k_3 = 0$) were first studied. Figure 2 displays a simulation in which $k_2 = 0{\cdot}1$ sec^{-1}, $t = 100$ sec and z varies from 0 to 0·3. The Lineweaver–Burk plot (Fig. 2(a)) apparently yields a set of lines converging on the ordinate and is thus characteristic of a competitive inhibition. Very careful examination of the set of points obtained for $z = 0{\cdot}3$ indicates a slight upward curvature but, within the limits of usual experimental errors (1–5 %), this curvature would remain totally undetectable. However, it is easy to compute that, at the end of the incubation period, the amount of enzyme irreversibly immobilized as complex EI^* is quite high (Table 1) and that the amount of product measured is very different from what would be measured if no EI^* complex were formed (rapidly reversible interaction). On the Dixon plot (Fig. 2(b)), the curvature is more readily detectable, mainly at low substrate concentrations but, these curves can again easily be confused with lines within the limits of the usual experimental errors. The lines converge and the "apparent K_i" value is about 0·1 K. It is interesting to note that a lower apparent K_i is obtained when only the points observed for large values of z ($z > 0{\cdot}15$) are used. When time is increased, and x and z remain constant, P_M/P also

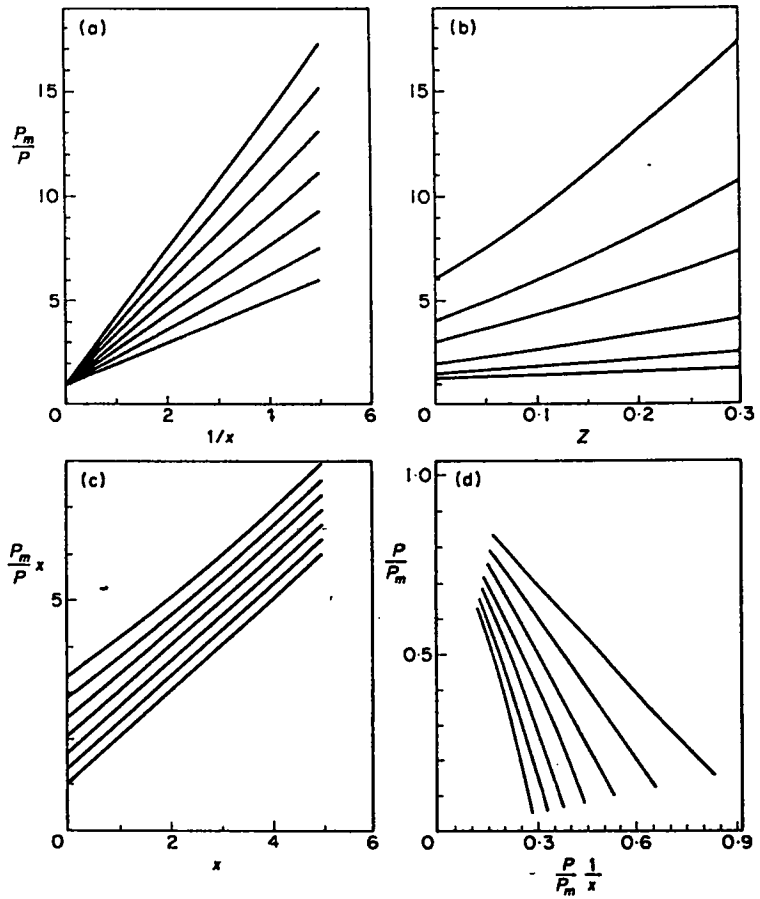

FIG. 2. Simulation of a competitive model. $q = 100$; $k_2 = 0{\cdot}1\ \text{sec}^{-1}$; $k_3 = 0$; $t = 100$ sec; z varies (a), (c) and (d) from 0 to 0·3. In (b), the values of x are 4, 2, 1, 0·5, 0·33 and 0·2.

TABLE 1

Proportion of enzyme immobilized as EI after 100 sec under the conditions of Fig. 2.*

	x	
z	1	0·2
0·05	0·22	0·33
0·3	0·73	0·87

increases but the patterns are essentially the same. No graph shows a stronger curvature than that observed on Fig. 2(b). The apparent K_i, computed from the Dixon plot, decreases with increasing time. For large values of t, the value of P/P_M becomes very small and, eventually, very close to zero. The value of z (i.e. the inhibitor concentration) must be decreased in order to obtain P_M/P ratios lower than 100. The Hanes plot might yield better indications of an abnormal situation (Fig. 2(c)): the lines which can be drawn through the points at low substrate concentrations ($x < 1$) clearly converge to *the right*, which is unexpected for any simple model of reversible inhibition. At higher substrate concentrations, the lines are very close to be parallel. Similarly, on the $P_M/P.x$ vs $[z]$ plot (not shown), the lines converge to the right. The Eadie–Hofstee plots also yield curves (Fig. 2(d)). The strongest curvatures are also observed for large z values. In this case, the lines which can be drawn through the points at low substrate and high inactivator concentrations extrapolate above $P/P_M = 1$ (for $P/P_M \cdot 1/x = 0$), a situation which is again unexpected for any simple model of reversible inhibition. In all cases (Lineweaver–Burk, Hanes, Dixon and Eadie–Hofstee graphs), it is very likely that in a real experimental situation, the curves will be mistaken for sets of parallel (Hanes and $P_M/P \cdot x$ vs z plots) or converging (Eadie–Hofstee, Lineweaver–Burk and Dixon plots) lines.

If the value of k_3 is not negligible, the situation is somewhat different. Figure 3 depicts the evolution with time of a system in which $k_2 = 1\ \text{sec}^{-1}$ and $k_3 = 0{\cdot}01\ \text{sec}^{-1}$. After 30 sec (Fig. 3(a)), the system has not reached the steady-state: term n is not negligible. Upward curvatures are detectable on the Hanes graph. Upward and downward curvatures are also clearly

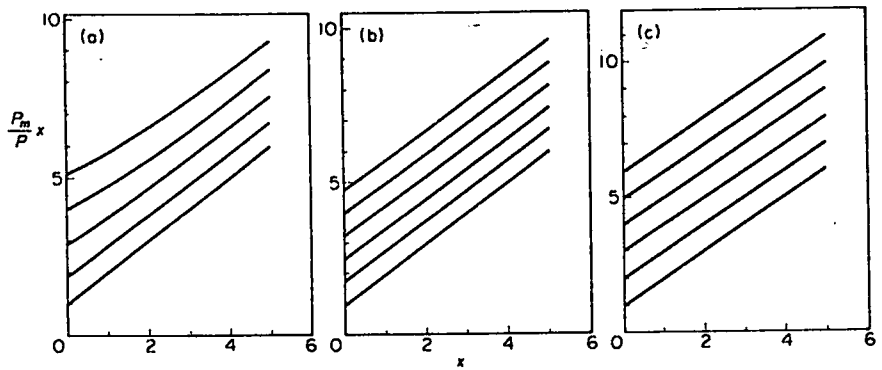

FIG. 3. Simulation of a competitive model, Hanes plots. $q = 100$, $k_2 = 1\ \text{sec}^{-1}$, $k_3 = 0{\cdot}01\ \text{sec}^{-1}$. (a) $t = 30$ sec, z varies from 0 to 0·2. (b) $t = 300$ sec, z varies from 0 to 0·05. (c) $t = 3000$ sec, z varies from 0 to 0·05.

detectable on the Dixon and Eadie–Hofstee plots, respectively (not shown). After 300 sec, the steady-state has been attained: term n is negligible but term m, although smaller than term l, cannot be neglected. The curves in the Hanes graph (Fig. 3(b)) can very easily be mistaken for a set of parallel lines. Similarly, the curvature of the lines in the Dixon and Eadie-Hofstee graphs becomes barely detectable. After 3000 sec, term m is negligible when compared to term l: the situation is that of a substrate competition and all plots yield true lines. The lines in the Hanes graph (Fig. 3(c)) are truly parallel. The values of the $(K_I)_{app}$ computed from the Dixon plot decrease from 0·056 K at $t = 30$ sec to 0.014 K at $t = 300$ sec and 0·0099 K at $t = 3000$ sec. This latter value is characteristic of a substrate competition (i.e. $k_3K/(k_2+k_3)$). If contact times shorter than 30 sec were used, the value of $(K_I)_{app}$ would increase and reach a limit close to K for extremely short contact times.

It should be emphasized that curvatures stronger than those depicted on Figs 2 and 3 were never obtained when a non-negligible value of k_3 was chosen.

MEDIUM VALUES OF q ($q = 1$). NON-COMPETITIVE MODEL

Very low values of k_3

As above, the EI^* complex irreversibly accumulates. The aspect of the Lineweaver–Burk, Hanes and Eadie–Hofstee graphs strongly depends upon the value of k_2. If k_2 is so high that very small inhibitor concentrations (very small z) must be used in order to obtain reasonable amounts of product, the contributions of complexes EI and ESI to the inhibition remain negligible (the proportion of these complexes would be non-negligible when compared to EI^* only if the time of contact were very short). Only E and EI^* are present, and EI^* accumulates with time. The observed pattern is competitive and P_M/P increases with time so that, when longer contact times are used, the value of z must be decreased. Under such conditions, no distinction can be made between a competitive and a non-competitive model. The fact had already been underlined in an earlier publication (Frère *et al.*, 1975*b*).

If k_2 is smaller, so that inhibitor concentrations close to K are used, time becomes the determining factor: for low values of t, ESI represents a sizable proportion of the inhibited enzyme, and the pattern is non-competitive. As t increases, EI^* accumulates and, eventually, ESI becomes negligible: the pattern becomes competitive.

Figure 4 depicts two extreme situations: on Fig. 4(a), only low amounts of EI^* have accumulated during the very short time of contact: after 30 sec,

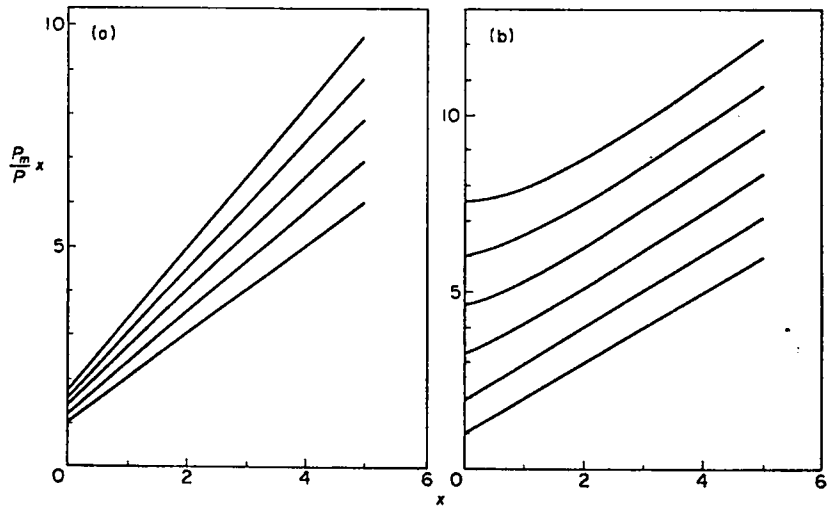

FIG. 4. Simulation of a non-competitive model, Hanes plots. $q = 1$, $k_2 = 0{\cdot}01\ \text{sec}^{-1}$, $k_3 = 0$. (a) $t = 30$ sec, z varies from 0 to 0·6. (b) $t = 2500$ sec, z varies from 0 to 0·3.

$[EI^*]/E_0 = 0{\cdot}09$ for $x = 0{\cdot}2$ and $z = 0{\cdot}6$ and 0·01 for $x = 5$ and $z = 0{\cdot}15$. Most of the inhibition is due to *EI* and *ESI*. On Fig. 4(b), most of the inactive enzyme is in the form EI^*: after 2500 sec, $[EI^*]/E_0 = 0{\cdot}993$ for $x = 2$ and $z = 0{\cdot}6$ and 0·22 for $x = 5{\cdot}0$ and $z = 0{\cdot}06$. In this latter case, $[EI]/E_0$ and $[ESI]/E_0 = 0{\cdot}007$ and 0·035, respectively. Again, on Fig. 4(b), a clear deviation from linearity occurs at low substrate concentrations and the lines which can be drawn for $[S]/Km < 2$ converge *to the right.*

Values of k_3 similar to k_2z

Again, the general pattern is determined by the value of k_2: if k_2 is very high, very low concentrations of inactivator must be used, and, as above, the pattern is competitive for any value of t. On the contrary, if k_2 is not very high, the three complexes *EI*, *ESI* and EI^* are still present after the steady-state has been established and the pattern is non-competitive for all values of t.

VERY LOW VALUES OF q ($q = 0{\cdot}01$). UNCOMPETITIVE MODEL

$k_3 \ll k_2z$

If the value of k_2 is very high, one can observe a competitive pattern as in the non-competitive model, even for low values of t. However, in the

present case, the value of k_2 must be much higher than in the non-competitive model, because the low value of q involves the formation of 100-fold more *ESI* than *EI*. The transformation of *EI* into *EI** must thus be extremely rapid to counterbalance this disadvantage and conserve conditions in which $[ESI] \ll [EI^*]$ (Table 2, example with $k_2 = 100\ \text{sec}^{-1}$). When the value of k_2 is not high enough to fulfill this condition, but still rather high, the pattern is non-competitive for low vlaues of t. The abcissa of the convergence point in the Lineweaver-Burk plot decreases with increasing time and, for large values of t, the pattern becomes competitive (Table 2, example with $k_2 = 1\ \text{sec}^{-1}$).

TABLE 2

Patterns obtained in an uncompetitive model ($q = 0{\cdot}01$) *when* $k_3 \ll k_2 z$

				Pattern		Abcissa of convergence point	
k_2	k_3	z_{max}	t	in L–B plot	in H plot	in L–B plot	in H plot
100	10^{-6}	10^{-4}	100	C	C†	0	$-\infty$
1	10^{-6}	0·06	30	NC	NC	−6	−0·24
		0·03	100	NC	NC	−1·7	−0·71
		0·01	500	NC	NC†	−0·25	−3·1¶
		0·003	1 000	NC	NC†	−0·17	−6·3¶
		0·001	5 000	C	C†	0	<−60
0·1	10^{-6}	0·1	30	UC–NC§	UC–NC‡	−40	>−0·06
		0·04	100	NC	UC–NC‡	−17	≃−0·1
		0·04	1 000	NC	NC	−1·7	−0·65
		0·01	5 000	NC	NC†	−0·3	−3·0¶
		0·01	10 000	NC–C‖	NC†	−0·05	−7·9¶
		0·002	20 000	C	C†	0	<−17

† Clear deviation from linearity for $x < 2$ and large values of z.

§‖ The convergence point is so far from § or so close to ‖ the ordinate axis that it would become quite difficult to make a choice in a real experiment.

‡ Convergence point very close to the ordinate axis ($0 \gg -0{\cdot}1$).

¶ When the points at low x clearly deviate from linearity, the lines are drawn with the points at $x \geqslant 2$. If the points at low S concentrations are also used to draw a line, the slope is lower, i.e. the convergence point is more negative and the graph closer to a "competitive" graph.

L–B plot: Lineweaver–Burk plot; H plot: Hanes plot.

Finally, with lower values of k_2, the pattern can be uncompetitive, non-competitive and competitive depending on whether the t value is low, intermediate or high, respectively (Table 2, example with $k_2 = 0{\cdot}1\ \text{sec}^{-1}$).

Values of k_3 similar to $k_2 z$

To obtain an apparently competitive pattern for small values of t, one needs a k_2/k_3 ratio of at least 1000, so that substantial inhibition is observed for very low values of z ($z < 0{\cdot}001$. i.e. $[I] < 0{\cdot}1\ K'$). For lower k_2/k_3 ratios ($k_2/k_3 \simeq 100$), and values of $[I]$ close to $0{\cdot}01\ K$ (i.e. $[I] \simeq K'$), the pattern is non-competitive for low values of t and remains so after establishement of the steady-state (Fig. 5). When the ratio k_2/k_3 is lower ($\simeq 10$), an uncompetitive pattern is observed for low values of t, which becomes non-competitive for larger values of t.

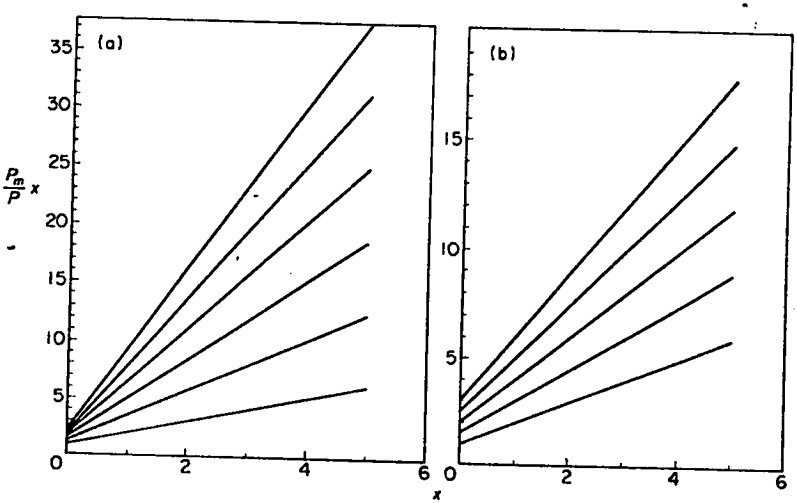

FIG. 5. Simulation of an uncompetitive model, Hanes plots. $q = 0{\cdot}01$, $k_2 = 1\ \text{sec}^{-1}$, $k_3 = 0{\cdot}01\ \text{sec}^{-1}$. (a) $t = 30$ sec, z varies from 0 to 0·06. (b) $t = 10\,000$ sec, z varies from 0 to 0·02.

Finally, if $k_2 \simeq k_3$, the values of z which should be used to obtain some EI^* complex are so high ($z \simeq 1$, i.e. $[I] \simeq 100\ K'$) that ESI becomes largely predominant and that the pattern remains uncompetitive whatever the time of contact.

It should be noted that, in all the simulations which have been performed, the curves obtained in the Lineweaver–Burk plots are very close to straight lines. Dixon and Hanes plots sometimes show a slight upward curvature and Eadie–Hofstee plots a slight downward curvature, similar to those seen on Fig. 2. The curvature is strongest when the inhibition is due to the accumulation of EI^*, but it would always remain undetectable under real experimental conditions. The Hanes plots exhibit the strongest deviations

from linearity at low substrate concentration and when an important proportion of enzyme accumulates as EI^*. However, these deviations from linearity might still remain difficult to detect in actual experimental conditions. A better indication that something unexpected is happening might be deduced from the fact that lines obtained at low S concentrations ($[S] \leq Km$) converge *to the right*. Similarly, when the Eadie–Hofstee plots are used, convergence of the lines on the *right* of the ordinate might indicate more clearly an unexpected irreversible reaction than a nearly undetectable deviation from linearity.

Discussion

In a gross qualitative manner, our simulations yield results in agreement with the logical expectations: the inhibition pattern which is observed reflects the nature of the complexes which are predominant throughout the duration of the incubation. If only complexes EI and EI^* are present, the pattern is competitive; if only ESI is present, the pattern is uncompetitive; and in the other cases (presence of the three complexes or of ESI and EI^*), the pattern is non-competitive. It is interesting to remember that the pattern can change with time, going from non-competitive to competitive, from uncompetitive to non-competitive or even from uncompetitive to competitive as EI^* accumulates.

The present description of our analysis has been, for practical reasons, limited to some well-defined values of the variables. Simulations with intermediate values have also been performed, but their results do not alter the conclusions presented above.

Quantitatively, however, the simulations yielded a rather unexpected result. In all cases, and although the equations are certainly not linear vs $[S]$, $1/[S]$ or $[I]$, all the Hanes, Lineweaver–Burk, Eadie–Hofstee and Dixon plots were quasi-linear. As noted above, the strongest curvatures were observed in Hanes, Eadie–Hofstee and Dixon plots, when the accumulation of EI^* became important. Even in these cases, these plots would certainly appear linear under actual experimental conditions. In some cases, however, the convergence point of the Hanes and Eadie–Hofstee lines might indicate that a simple, reversible model is not verified. Thus, under conditions in which a large portion of the enzyme is irreversibly immobilized as EI^*, it might be difficult to detect it by the usual graphical methods. Hence the importance of verifying that the experiment is performed under true steady-state conditions cannot be stressed with too much insistance.

It is interesting to note that similar results have recently been obtained in a very different field: the interaction between hormone (H) and isolated

receptors (R) can sometimes be represented by the simple scheme

$$H + R \underset{k-1}{\overset{k+1}{\rightleftharpoons}} HR \xrightarrow{k_2} HR^*.$$

Under these conditions, measurement of the "bound" hormone in fact represents $[HR]+[HR^*]$. If Scatchard plots are thus constructed, they are linear for a wide range of hormone concentrations. Computer simulations show that the plots only deviate from linearity for high values of the "bound" hormone concentrations. These deviations are slight and might easily escape detection. Not surprisingly, the apparent "dissociation constant" of the "hormone receptor complex" calculated on the basis of a simple, rapidly reversible equilibrium, decreases with increasing times of contact (Ketelslegers, 1982). These observations again indicate that non-steady-state or non-equilibrium situations might remain undetected when the usual plots are mistakenly used for their study.

The work has been supported by the National Institutes of Health, Bethesda, Maryland (contract no 2 R01 13364-05), the Fonds de la Recherche Scientifique Médicale, Brussels (contract 3.4501.79) and the Actions concertées, Brussels (convention 79/84-11).

The authors wish to thank Dr K. Tipton for interesting comments and suggestions.

REFERENCES

BARNETT, M. J. (1973). *Biochim. biophys. Acta* **304**, 332.
CHA, S. C. (1975). *Biochem. Pharmacol.* **24**, 2177.
CHA, S. C., AGARWAL, R. P. & PARKS, R. E., JR. (1975). *Biochem. Pharmacol.* **24**, 2187.
FRÈRE, J. M., LEYH-BOUILLE, M., GHUYSEN, J. M. & PERKINS, H. R. (1974*a*). *Eur. J. Biochem.* **50**, 203.
FRÈRE, J. M., GHUYSEN, J. M., REYNOLDS, P. E., MORENO, R. & PERKINS, H. R. (1974*b*). *Biochem. J.*, **143**, 241.
FRÈRE, J. M., GHUYSEN, J. M. & IWATSUBO, M. (1975*a*). *Eur. J. Biochem.* **57**, 343.
FRÈRE, J. M., GHUYSEN, J. M. & PERKINS, H. R. (1975*b*). *Eur. J. Biochem.* **57**, 353.
FRÈRE, J. M., GHUYSEN, J. M., DEGELAEN, J., LOFFET, A. & PERKINS, H. R. (1975*c*). *Nature (Lond.)* **258**, 168.
FRIEDEN, C. (1970). *J. biol. Chem.* **245**, 5788.
HENDERSON, P. J. F. (1972). *Biochem. J.* **127**, 321.
IZAKI, K. & STROMINGER, J. L. (1968). *J. biol. Chem.* **243**, 3193.
KETELSLEGERS, J. M. (1982). *Thèse d'Agrégation*, Université de Liège, Belgium.
LEYH-BOUILLE, M., COYETTE, J., CHUYSEN, J. M., IDCZAK, J., PERKINS, H. R. & NIETO, M. (1971). *Biochemistry* **10**, 2163.
LEYH-BOUILLE, M., NAKEL, M., FRÈRE, J. M., JOHNSON, K., GHUYSEN, J. M., NIETO, M. & PERKINS, H. R. (1972). *Biochemistry* **11**, 1290.
MARTIN, H. H., MASKOS, C. & BURGER, R. (1975). *Eur. J. Biochem.*, **55**, 465.
MORRISSON, J. F. (1969). *Biochim. biophys. Acta* **185**, 269.
OPPENHEIM, O., KOREN, R. & PATCHORNIK, A. (1974). *Biochem. biophys. Res. Commun.* **57**, 562.
UMBREIT, J. N. & STROMINGER, J. L. (1973). *J. biol. Chem.* **248**, 6767.
YOCUM, R. R., BLUMBERG, P. M. & STROMINGER, J. L. (1974). *J. biol. Chem.* **249**, 4863.